Reports

Laser Method for Synthesis and Processing of Continuous Diamond Films on Nondiamond Substrates

J. NARAYAN,* V. P. GODBOLE, C. W. WHITE

A laser method based upon carbon ion implantation and pulsed laser melting of copper has been used to produce continuous diamond thin film. Carbon ions were implanted with ion energies in the range of 60 to 120 keV, and doses of 1.0×10^{18} to 2.0×10^{18} ions cm^{-2}. The ion-implanted specimens were treated with nanosecond excimer laser pulses with the following parameters: energy density, 3.0 to 5.0 J cm^{-2}; wavelength, 0.308 μm; pulse width, 45 nanoseconds. The specimens were characterized with scanning electron microscopy (SEM), x-ray diffraction, Rutherford backscattering/ion channeling, Auger, and Raman spectroscopy. The macroscopic Raman spectra contained a strong peak at 1332 cm^{-1} with full width at half maximum of 5 cm^{-1}, which is very close to the quality of the spectra obtained from single-crystal diamond. The selected area electron diffraction patterns and imaging confirmed the films to be defect-free single crystal over large areas of up to several square micrometers with no grain boundaries. Low voltage SEM imaging of surface features indicated the film to be continuous with presence of growth steps.

GRAPHITE, WHICH IS THE THERMODYNAMICALLY stable phase of carbon at room temperature, can be converted into diamond at high pressure (200 kbar) and high temperature (4273 K) (*1, 2*). Diamond has been grown as an equilibrium phase from liquid metal solutions at lower pressures and temperatures. By the use of a metallic catalyst such as nickel, cobalt, iron, tantalum, and chromium, transformation rates can be increased, and temperature and pressure can be reduced to 2300 K and 70 kbar, respectively (*1–3*). Diamond can be grown at subatmospheric pressure and temperature from hydrocarbon gases in the presence of atomic hydrogen. Diamond thin films have been successfully grown by a variety of low-pressure and low-temperature chemical vapor deposition (CVD) methods such as filament-assisted CVD, plasma (microwave, radio frequency, direct-current discharge) CVD, and combustion flames (*4–6*). In these methods, typically a mixture of hydrocarbons such as CH_4 and C_2H_2 and hydrogen (98 to 99.5% by volume) is passed over the heated (973 to 1273 K) substrates such as silicon, molybdenum, nickel, copper, tungsten, tantalum, titanium, boron nitride, silicon carbide, silicon nitride, tungsten carbide, sapphire, or silica glass. During the CVD process, both diamond and graphite are deposited. However, preferential etching of graphite by hydrogen leaves diamond crystallites which continue to grow to form polycrystalline films. These polycrystalline films contain a high density of defects such as dislocations, twins, stacking faults, and grain boundaries. Such films, while useful for coating applications, are not suitable for fabrication of electronic devices, because the defects provide traps and recombination centers for charge carriers (*7*). Single-crystal diamond thin films have been grown epitaxially only on diamond substrates, where all three axes of the film are aligned with respect to the substrate (*8*).

We have used a laser method, which is novel to the best of our knowledge, to produce continuous, diamond thin films on nondiamond substrates such as copper. In this method, the substrate is implanted with C^+ ions at room temperature to a high dose, and the implanted specimens are subsequently irradiated with nanosecond laser pulses to melt and rapidly solidify (laser anneal) the implanted regions of the specimens at ambient temperature and pressure (*9*). During this process, it is envisaged that implanted carbon atoms cluster and form the diamond phase. Thin films grown by this method have been characterized by SEM, transmission electron microscopy (TEM), x-ray diffraction, Rutherford backscattering/channeling, Auger, and Raman spectroscopy.

Polycrystalline and single-crystal copper (100) and (111) specimens (with dimensions 10 by 10 mm) were chemically polished and implanted with carbon ions (dose, 1.0×10^{18} to 2.0×10^{18} ions cm^{-2}; energy, 60 to 120 keV) at room temperature. The as-implanted specimens were irradiated with laser pulses to melt and rapidly solidify the implanted regions. The laser parameters used in the present experiments were as follows: wavelength (λ), 0.308 μm; pulse duration (τ), 45 ns; and energy density (E), 3.0 to 5.0 J cm^{-2}. It should be mentioned that other beam sources, such as electrons and ions, can also be used as long as the beam parameters are adjusted so that optimum requirements for melting and solidification are met. Similarly, carbon can be deposited on atomically clean substrates followed by deposition of a thin copper film, by means of physical vapor deposition techniques such as in situ laser evaporation. The ion-implanted specimens were studied in detail with transmission electron microsco-

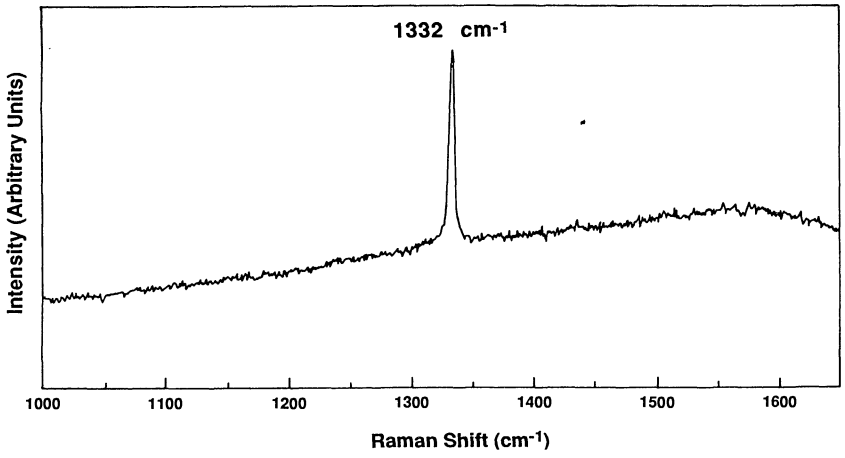

Fig. 1. Raman spectrum from ion-implanted (60 keV, 1.0×10^{18} ions cm^{-2}) and laser-annealed (E = 3.0 J cm^{-2}) specimen. The Raman peak at 1332 cm^{-1} with a FWHM of 5 cm^{-1} is indicative of high-quality diamond film.

J. Narayan and V. P. Godbole, Department of Materials Science and Engineering, North Carolina State University, Raleigh, NC 27695–7916.
C. W. White, Solid State Division, Oak Ridge National Laboratory, Oak Ridge, TN 37831.

*Present address: National Science Foundation, Division of Materials Research, Washington, DC 20550.

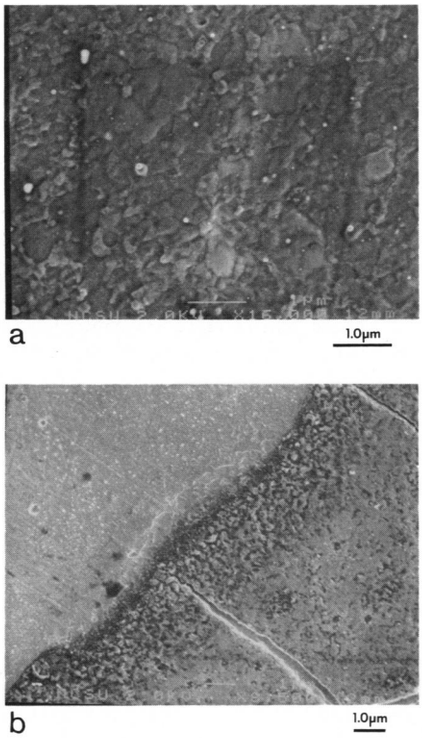

Fig. 2. SEM micrographs at low voltage of 2.0 keV: (**a**) smooth film with growth steps; and (**b**) multiple (five) pulses at 3.0 J cm^{-2} result in film cracking. The micrograph also shows boundary between laser-treated and as-implanted region.

py (Philips EM-430, Hitachi S-800, JEOL 200 CX), low voltage–scanning electron microscopy (JEOL-6400 equipped with field emission gun), Rutherford backscattering (RBS)/ion channeling, x-ray diffraction, Auger spectroscopy, and Raman measurements. The Raman spectra were recorded with a SPEX triple monochromator equipped with a photo-multiplier and photon counting electronics. The Raman data were collected in photon counting mode using the 5145 Å line from an Ar^+ ion laser as excitation source and in 180° backscattering geometry. A slit width of 2 mm was used for macro-Raman measurements on the ion-implanted and laser-annealed specimens, so peak width of the spectrum is dispersion-limited by 2 cm^{-1}.

Macroscopic Raman measurements were obtained on 2 by 10 mm area of the ion-implanted and laser-treated copper specimen (Fig. 1). The Raman active mode appears at 1332 cm^{-1} with a peak width (FWHM) of 5 cm^{-1}. Under similar experimental conditions, spectra from (100) single-crystal bulk diamond substrates contained a peak at 1332 cm^{-1} with FWHM of 3 to 4 cm^{-1}. An absence of peaks at 1550 cm^{-1} (nondiamond carbon) and at 1133 cm^{-1} (nanocrystalline diamond) is indicative of the high quality of diamond film. Figure 2a shows a SEM electron micrograph taken at 2.0 keV, revealing clearly surface features of the diamond film. The surface morphology shows growth steps and confirms the continuous nature of the film. The SEM micrograph in Fig. 2b was obtained after multiple (in this case, five) laser pulses, which resulted in the formation of cracks in the film. The thermal stresses are generated because of the differences in thermal expansion coefficients between diamond (α-linear = 5.0 × 10^{-6} K^{-1}) and copper (2.0 × 10^{-5} K^{-1}) at 1273 K, and this leads to cracking of the film.

The specimens for TEM were prepared by polishing away the copper substrate and lifting off the diamond layer on a molybdenum grid using dilute nitric acid. Figure 3a is a bright-field TEM micrograph indicating absence of defects such as twins and stacking faults (7), which are normally observed in CVD diamond films. Moiré fringes are observed owing to differences in lattice constants between diamond (a_o = 3.615 Å) and copper (a_o = 3.568 Å), in the regions of the film where copper was present underneath the diamond film. The corresponding selected area diffraction pattern in Fig. 3b shows a sharp spot pattern characteristic of ⟨111⟩ oriented film. The double diffraction spots are from residual copper layer on which diamond layer has grown. A complete alignment between diamond and copper diffraction spots indicates the epitaxial nature of the diamond film on the single-crystal copper substrate over several square micrometers. If laser parameters are not fully optimized, polycrystalline substrates give rise to polycrystalline films, as revealed by characteristic selected area diffraction patterns for diamond (Fig. 3c). The thickness of the diamond film was estimated to be 500 Å which was consistent with estimated thickness of 560 Å from ion implantation dose of 1.0 × 10^{18} ions cm^{-2} (thickness = dose divided by 1.76 × 10^{23} atoms cm^{-3}).

The x-ray diffraction results contained characteristic peaks corresponding to 111 (d = 2.06 Å), 200 (d = 1.808 Å), 220 (d = 1.26 Å), 311 (d = 1.076 Å), and 400 (d = 0.891 Å) reflections. The RBS and Auger results showed that in room temperature–implanted specimens the carbon peak is at 700 Å, which was found to sharpen and move towards the surface with the number of laser pulses, and attain uniform carbon distribution in the region where diamond film is envisaged to form.

Carbon ion implantation at room temperature as well as at higher temperatures (973 to 1073 K) alone did not result in the formation of diamond phase. Pulsed laser melting and rapid solidification was found to be necessary for the formation of diamond phase. We have also investigated the deposition of diamond films by hot filament CVD (filament temperature, 2273 K; substrate temperature, 1073 K; and CH_4/H_2,

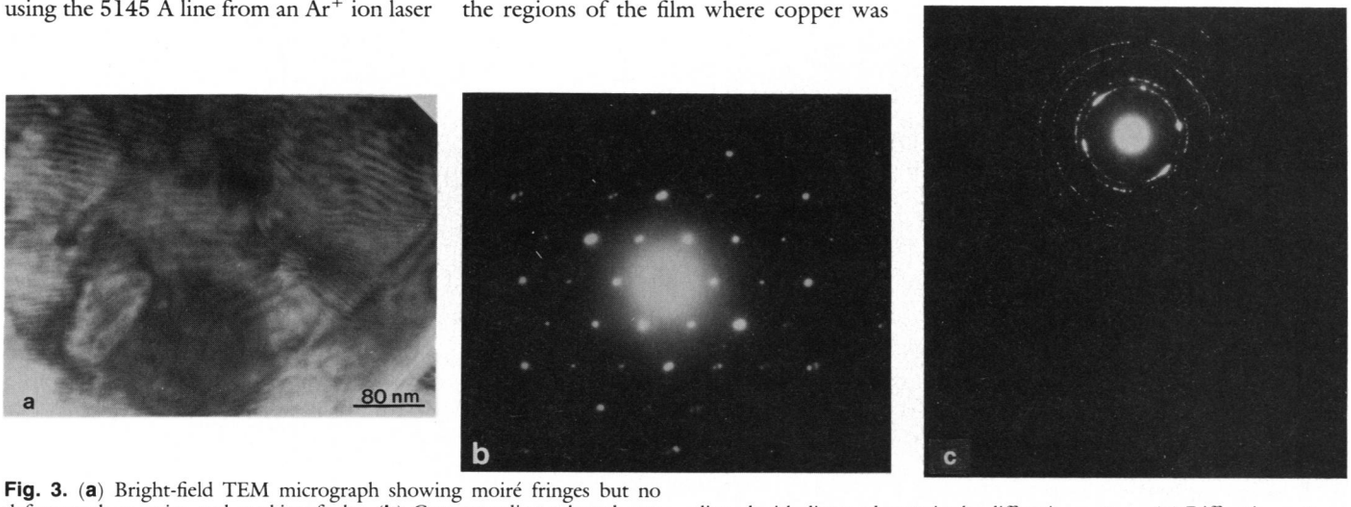

Fig. 3. (**a**) Bright-field TEM micrograph showing moiré fringes but no defects such as twins and stacking faults. (**b**) Corresponding selected area diffraction indicating ⟨111⟩ film orientation. The substrate Cu spots are aligned with diamond spots in the diffraction pattern. (**c**) Diffraction pattern from polycrystalline diamond film.

1.0/100) on laser-deposited cubic boron nitride on copper substrates. High-quality polycrystalline films were obtained on stainless and tool steels with c-BN and WC buffer layers (*10*).

To investigate the mechanism of diamond phase formation, we have simulated thermal effects of nanosecond laser irradiation on carbon-doped copper substrates by solving the one-dimensional heat flow equation and taking into account the phase changes occurring at the surface of the irradiated solid. The temperature-dependent optical and thermophysical properties of copper and the presence of nonlinear boundary conditions make an analytical solution of this problem intractable. Thus, numerical simulation techniques have to be applied to accurately determine the thermal history of the irradiated surface.

We have employed an extremely accurate finite difference technique developed by Singh and Narayan (*11*) to solve the heat flow equation with appropriate boundary conditions. As a first approximation, we have assumed that the thermal properties of copper are not strongly affected by carbon implantation. Even if this assumption is not fully valid, the thermal effects of laser irradiation on copper would be very similar, except for the shifting of the absolute energy density values. The thermal and the optical properties used in these calculations have been outlined in Table 1 (*12*). Copper possesses very high thermal conductivity (4.0 W cm^{-1} K^{-1} at 300 K), which decreases steadily with increasing temperature, followed by a sharp decrease upon melting of the material. The relatively low plasma frequency of copper allows excellent coupling of the laser energy with the solid. The reflectivity of copper also undergoes a sharp transition upon melting. This leads to very interesting near-surface effects during laser irradiation at energy densities slightly above the melt threshold. Figure 4, a and b, show, respectively, the melt depth and surface temperature as a function of time for carbon-doped copper targets irradiated with 45-ns excimer laser pulses, with an energy density for the pulse corresponding to 3.0, 4.0, and 5.0 J cm^{-2}. The pulse shape was assumed to be trapezoidal with linear rise and decay times corresponding to 5 and 15 ns, respectively. The slope of the melting curves correspond to the melt-in and solidification velocities of the liquid-solid interface formed after laser irradiation. The figure shows that the surface reaches the melting temperature within very short times; however, more laser energy has to be deposited before the melt interface starts to propagate inside the bulk of the solid. This delay is attributable to the sudden increase in the reflectivity of the solid upon melting. The delay in melt propagation is very large (approximately 15 ns at 3 J cm^{-2}) at laser energy densities just above the threshold for melting. The maximum melt depth increases with energy density, and changes from approximately 2300 Å to 9000 Å when energy density is increased from 3 to 5 J cm^{-2}.

A very interesting feature of this calculation is the extremely high solidification velocities (25 to 30 m s^{-1}) of copper after the termination of the laser pulse. The extremely high solidification velocities are the result of the high thermal conductivity of the solid. The diamond phase is envisaged to nucleate during rapid solidification and epitaxial film is formed on copper in which carbon is relatively insoluble. It is interesting to note that, while the near-surface layers (<1 μm thick) melt during pulsed laser irradiation, bulk of the substrate remains close to the ambient temperature. This feature lends itself to low-temperature processing of diamond films, an important consideration for coating and electronic device applications.

We have also grown thick diamond films using HFCVD (hot filament CVD) on these substrates and found them to be single crystals. This method should be applicable to other lattice- and plane-matched substrates having low solubility for carbon. The present method is ideally suited for making isotopically pure diamond containing ^{12}C, ^{13}C, or a combination of the two. The diamond layer can also be doped in a controlled way with either *p*- or *n*-type dopants by adjusting the implanted dose and energy of the dopant ions.

Table 1. Thermal and optical properties used in numerical simulations of thermal effects caused by laser irradiation

Thermal conductivity (W cm^{-1} K^{-1})	$4.1 - 6.5714 \times 10^{-4}$ $(T - 200)$ for $T < 1357$ K 1.8 for $T > 1357$ K
Specific heat capacity (J cm^{-3} K^{-1})	$3.4496 + 9.75 \times 10^{-4}$ $(T - 300)$ for $T < 1357$ K 4.4792 for $T > 1357$ K
Melting temperature	1357 K
Latent heat of fusion (J cm^{-3})	1840.05
Reflectivity	0.364 (solid) 0.73 (liquid)
Absorption coefficient (cm^{-1})	7.01×10^5

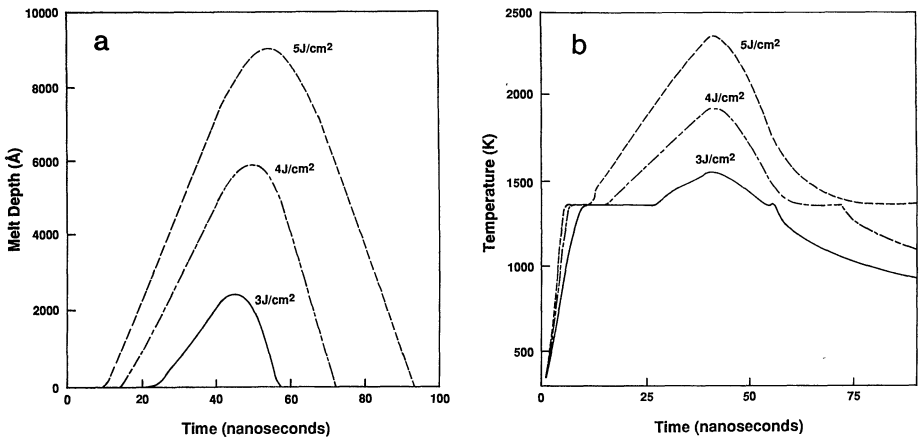

Fig. 4. Melt depth (**a**) and surface temperature (**b**) as a function of depth for 45-ns excimer laser (λ = 0.308 μm) pulses. Parameters used in the calculations are given in the Table 1.

REFERENCES AND NOTES

1. E. P. Bundy, H. T. Hall, H. M. Strong, R. J. Wentorf, Jr., *Nature* **176**, 51 (1955).
2. P. W. Bridgman, *Sci. Am.* **193**, 42 (November 1955).
3. R. C. DeVries, *Annu. Rev. Mater. Sci.* **17**, 161 (1987).
4. S. Matsumoto and Y. Matsui, *J. Mat. Sci.* **18**, 1785 (1983).
5. J. C. Angus and C. C. Hayman, *Science* **241**, 1823 (1988).
6. W. A. Yarbrough and R. Messier, *ibid.* **247**, 688 (1990).
7. J. Narayan, *J. Mater. Res.* **5**, 2414 (1990); _____, A. R. Srivatsa, K. V. Ravi, *Appl. Phys. Lett.* **54**, 1659 (1988); J. Narayan, A. R. Srivatsa, M. Peters, S. Yokota, K. Ravi, *ibid.* **53**, 1823 (1988).
8. M. W. Geis, *Mater. Res. Soc. Proc.* **162**, 15 (1990).
9. C. W. White, J. Narayan, R. T. Young, *Science* **204**, 461 (1979). It should be noted that the key to transformation of carbon to diamond in the present experiments is the fast quenching associated with pulsed laser annealing, whereas the continuous laser experiments of Fedoseev *et al.* [*Carbon* **21**, 237 (1983); *ibid.*, p. 243] did not achieve optimum quenching rates.
10. J. Narayan *et al.*, unpublished.
11. R. K. Singh and J. Narayan, *Mater. Sci. Engr. B* **3**, 217 (1989).
12. Y. S. Touloukian and C. Y. Ho, *Thermophysical Properties of Matter* (Plenum Press, New York, 1970), vols. 1 and 2; *American Institute of Physics Handbook* (McGraw-Hill, New York, 1963); M. F. von Allmen, in *Physical Processes in Laser-Materials Interactions* M. Bertolotti, Ed. (Plenum Press, New York, 1982), p. 49.

13. Scientific and technical discussions with M. Paesler, P. Russell, R. Singh, K. Jahncke, P. Tiwari, S. Pramanick, and M. Vellaikal are gratefully acknowledged. Part of this research was supported by the U.S. Army Research Office, and one of us (C.W.W.) was supported by the Division of Materials Sciences (DE-AC05-840R21400), Department of Energy.

12 March 1991; accepted 20 March 1991